TECHNICAL RESEARCH REPORT

The Performance of a Deformable-Membrane Tactile Sensor: Basic Results on Geometrically-Defined Tasks

by D. Hristu, N.J. Ferrier, R.W. Brockett

CDCSS T.R. 99-4
(ISR T.R. 99-53)

The Center for Dynamics and Control of Smart Structures (CDCSS) is a joint Harvard University, Boston University, University of Maryland center, supported by the Army Research Office under the ODDR&E MURI97 Program Grant No. DAAG55-97-1-0114 (through Harvard University). This document is a technical report in the CDCSS series originating at the University of Maryland.

Web site http://www.isr.umd.edu/CDCSS/cdcss.html

The performance of a deformable-membrane tactile sensor: basic results on geometrically-defined tasks.[1]

Dimitris Hristu[2]
University of Maryland
College Park, MD 20712
hristu@isr.umd.edu

Nicola Ferrier
University of Wisconsin
Madison, WI 53706
ferrier@engr.wisc.edu

Roger W. Brockett
Harvard University
Cambridge, MA 02138
brockett@hrl.harvard.edu

Abstract

The limitations of rigid fingertips in the precise and algorithmic study of manipulation have been discussed in many works, some dating back more than a decade. Despite that fact, much of the work in dexterous manipulation has continued to use the "point-contact" model for finger-object interactions. In fact, most of the exsisting tactile sensing technologies are not adaptable to deformable fingertips. In this work we report on experimental results obtained with a deformable tactile sensor whose properties are well-suited to manipulation. The results presented here show that the sensor described provides a rich set of tactile data.

1 Introduction

In this work we describe a deformable image-based tactile sensor whose output is an approximation of the tactile surface itself. We present a set of basic tactile sensing experiments designed to demonstrate aspects of the sensor's performance. The ability of our sensor to deform while accurately localizing contact(s) makes it a promising tool for use in dexterous manipulation and other applications.

Tactile sensors have been widely used in manipulation tasks [19], edge following [2], as well as automatic grasping [3] and compliance control [7]. One of the disadvantages of conventional tactile sensors is that they are inherently two-dimensional, meaning that they sense a pressure distribution over their surface but provide little or no information on possible deformations of the surface itself. With few exceptions ([22], [24]), tactile arrays are typically mounted against a rigid backing and covered with a thin rubber layer to provide friction. This rigidity limits the degree to which such sensors can be used in the study of manipulation tasks [5]. In addition, most of the existing tactile arrays are flat, so they must be mounted on flat or cylindrical fingertips. Shimoga and Goldenberg explored different ways of constructing non-rigid fingertips [26, 27]. Various materials including foam, rubber, powder and gel were investigated. The gel-filled membrane showed best overall performance in terms of attenuation of impact forces, conformability, strain dissipation, and reality factors. The compliant fingertips used this paper most closely resemble the gel-filled fingertip used by Shimoga.

Over the last two decades, tactile sensing research has focused on the development of technology and devices that attempt to endow robots with some of the dexterity that humans possess. Everyday experience as well as analysis of the kinematics of manipulation and grasping [17, 21] suggest that contact forces and locations are the most important geometric parameters for manipulation and it is precisely those parameters that most tactile sensors are designed to measure. We will briefly state some of the most important examples of tactile sensing technologies, as they pertain to manipulation. See [14] for a comprehensive review.

Many of the tactile sensors in existence use piezoresistive [12, 28] or capacitive arrays [9, 14] of pressure-sensitive elements which when in contact with an object, can provide information on the location of the contact and its pressure distribution. Capacitive tactile arrays are usually preferred over their piezo-electric counterparts due to their higher sensitivity, linear response and lack of hysteresis. Optical tactile sensors are an alternative to tactile arrays and been developed for contact localization, including [23], [1] and [20]. Other image-based tactile sensors are described in [6] and [10]. In [25], [4] and [8] "intrinsic" tactile sensing is explored, where knowledge of a (rigid) fingertip's shape is used in conjunction with force-torque

[1]This work was funded by the followging grants: Army DAAG 55 97 0114, NSF EEC 94 02384 and Army DAAL 03-92- G 0115.

[2]This work was done while the author was with the Division of Engineering and Applied Sciences at Harvard University, Cambridge, MA.

sensors. A significant amount of work has involved dynamic tactile sensing. Dynamic tactile sensors (e.g. [15, 13, 18]) typically measure transient contact effects such as vibrations, stress changes and slip.

2 A 3-D Deformable Tactile Sensor

Figure 1 shows the deformable tactile sensor that has been developed in the Harvard Robotics Lab as a result of a decade-long collaborative effort. A complete description of the sensor and its operation can be found in [10]. The sensor consists of a metal housing and a roughly elliptical latex membrane which provides an area of contact. A clear, fluid-like gel fills the membrane, sealed from the rest of the assembly by a transparent window. A grid of dots is drawn at precisely computed locations on the inner surface of the membrane. A metal fingernail serves to provide support for the membrane when it is being deformed by contact. The fingertip is approximately $6.2cm$ long and has a diameter of $2cm$ at its base. A schematic is shown in Fig. 2. The sensor's metal housing holds a camera with a diameter of $7.5mm$ and a fiber optic cable that illuminates the interior surface of the membrane. The camera is connected to an image acquisition board which captures images of the grid of dots on the membrane. Typical images are shown in Fig. 3. The image size that was used was 192×120 pixels. The sensor has mechanical properties that are much better suited to manipulation than those of conventional robotic sensors. In particular, the use of a fluid-supported membrane ([5]) allows local deformations (caused by contact with an object) to be distributed throughout the enclosed volume, because of the constant pressure of the fluid inside. This is in contrast to materials that obey Hooke's law (i.e. rubber-covered rigid fingertips) and allows the fingerpad to locally "wrap around" the object at a contact. Mechanically, the sensor acts much like a human fingertip (albeit more compliant) and is very effective in providing grasp stability.

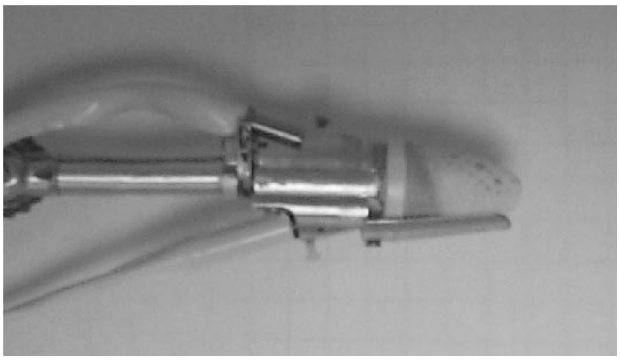

Figure 1: The tactile sensor.

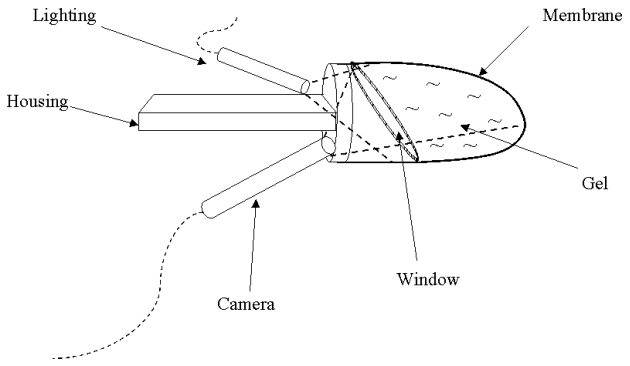

Figure 2: Tactile sensor schematic.

Figure 3: Camera view of membrane: (a) undeformed (b) in contact with an object.

3 Membrane Shape Reconstruction

The locations of the dots on the membrane are known a priori. When the fingertip comes in contact with the environment, the membrane deforms and the camera observes a change in the projections of the grid of dots onto the image plane (as in Fig. 3-b). Projective geometry tells us that there exist an infinity of solutions for the new three-dimensional coordinates of the dots. Under deformation, the portion of the membrane which is not in contact will assume a shape that minimizes its elastic energy. In addition, the volume enclosed by the membrane remains constant, and the boundary of the membrane is fixed. These constraints, together with some genericity assumptions on the grid of dots are sufficient to obtain a solution for the three-dimensional coordinates of the grid. The algorithm used to accomplish this (termed "the reconstruction algorithm") is presented in [10, 11].

Briefly, the reconstruction algorithm uses images such as the one in Fig. 3 to produce a three-dimensional approximation of the membrane surface, in the form of a 13×13 mesh that corresponds to a $4cm^2$ area on the fingerpad. The steps of the membrane reconstruction algorithm are depicted in Fig. 4. Details of the algorithm are presented elsewhere [11]. A reconstruction example is shown in Fig. 5, corresponding to a human fingertip lightly touching the membrane. The coordinates of the grid are measured with respect to an inertial frame whose origin at the center of the CCD array in the camera and whose z-axis is perpendicular

to that array. "Crossed" points represent the undeformed location of the grid. The straight line through the grid is drawn through the centroid of the area of contact (see Sec. 4). The reconstruction algorithm assumes that membrane deformations are "small".

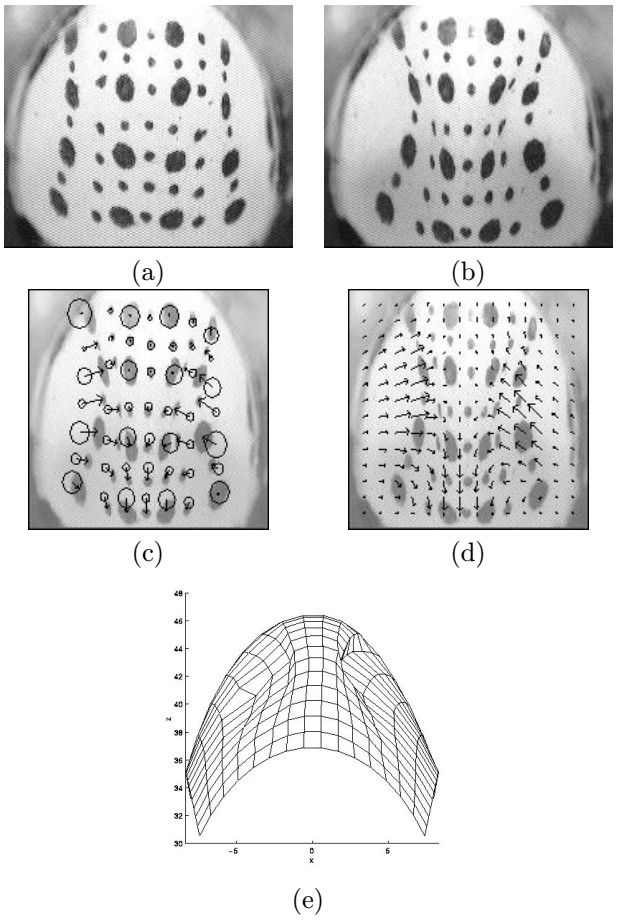

Figure 4: The fingertip operation: (a) a pattern of dots is drawn on the interior of a fluid-filled membrane. (b) The membrane deforms when in contact with objects. (c) Image data of the displacement of the pattern of dots is used to interpolate a flow field, (d). The image flow field, along with other constraints enable reconstruction of the 3D shape of the deformed membrane (e).

In addition, the algorithm involves a significant amount of computation and image processing. On a dual $400MHz$ Pentium PC the maximum rate of performing this reconstruction is $15Hz$ using a 5×5 grid of dots on the membrane and a 13×13 interpolated grid to approximate the fingerpad surface. This rate is low compared to those that can be achieved with traditional tactile sensors, however the deformable sensor provides a much richer description of a contact. Using denser grids for the membrane surface increases the precision of the tactile data as well as the computation time for a single reconstruction.

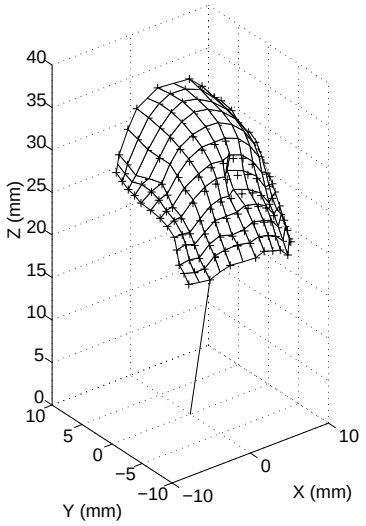

Figure 5: Tactile sensing example.

4 Tactile Sensor Performance

In the following, we describe a set of tactile sensing experiments that were designed to demonstrate the performance of our tactile sensor. In these experiments, we were interested in evaluating the sensor's accuracy (in contact localization tasks), spatial resolution, reconstruction accuracy and curvature discrimination.

Contact Localization: From the three-dimensional reconstruction of the fingerpad we can estimate which portion of the membrane is in contact with an object. Consider the reconstruction example of Fig. 5. By computing the displacement along the inward-pointing normal for each point on the grid, we can identify the points which are part of a contact. Figure 6 shows typical results obtained with this method when a pencil tip is pressed lightly against the fingerpad. The graph shows a peak forming around

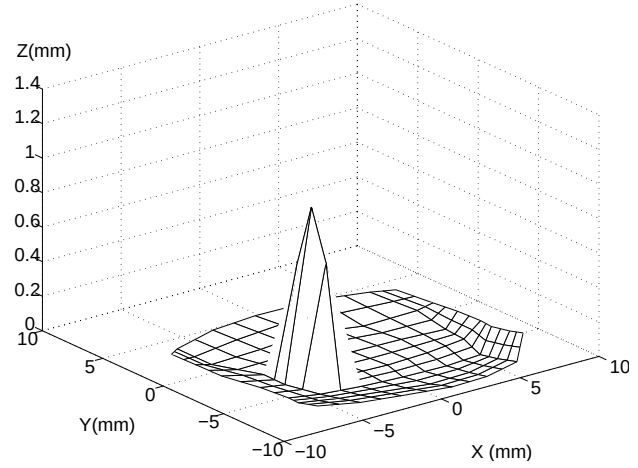

Figure 6: Contact detection.

the area of contact from which we can determine that the pencil was pressed about $1mm$ into the membrane. The area of contact included 14 grid points with their centroid at $(-4.5mm, -3.7mm, 22.2mm)$ measured in a coordinate frame located at the end of the distal link. In the following, we will use the terms "contact" or "contact location", to refer to the centroid of the area of contact. Our tactile sensor is able to simultaneously detect multiple areas of contact, as shown in Fig. 7. The minimum inward displacement that can be detected is $0.5mm$.

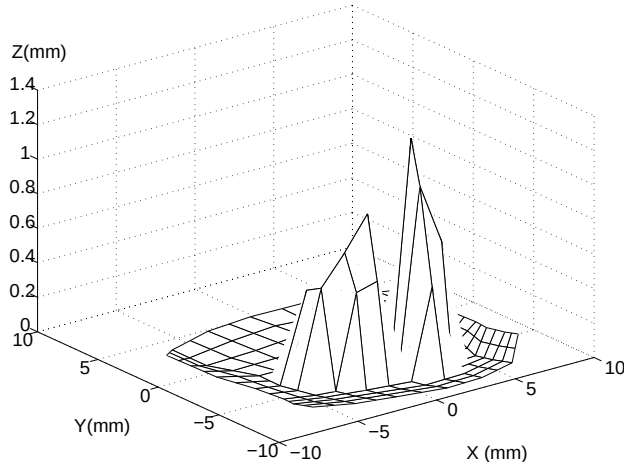

Figure 7: Double contact detection.

Constant lighting conditions and sufficient image resolution are necessary in order for the reconstruction algorithm to repeatably locate the projections of the membrane dots on the image. The following experiment was performed in order to measure the noise level associated with detecting dot projections in the camera image: The membrane was kept motionless, 100 images like the one shown in Fig. 3 were taken and the centroid of each dot was computed. The standard deviation of the noise was approximately 0.70 pixels and 0.61 pixels in the horizontal and vertical directions respectively. If we identify a contact by the centroid of all grid points that are part of that contact then the error (due to lighting noise) in computing the coordinates of the contact had a norm less than $0.1mm$.

Accuracy under Small Deformations: The accuracy of the reconstructed grid depends on the spatial density of dots drawn on the membrane. Currently a 5×5 grid is used, covering an area of $4cm^2$. In order to measure the accuracy with which the sensor can localize contact over its surface under small deformations, the following experiment was performed. The sensor was mounted on an apparatus (pictured in Fig. 8) which allows an indenter to be brought in contact with the fingerpad. The indenter is mounted on a 5 degree-of-freedom assembly so that it can always be

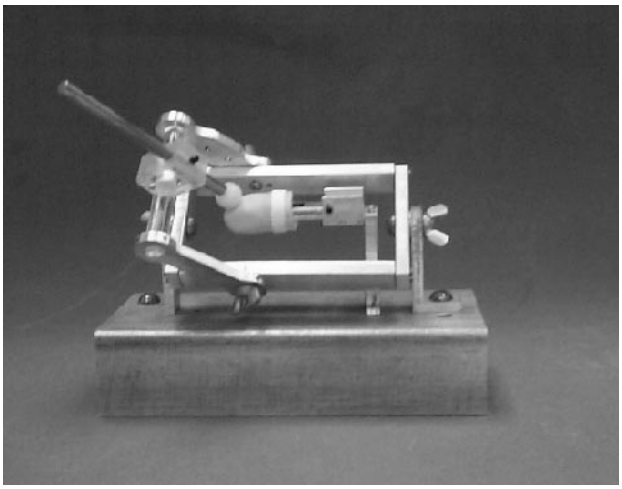

Figure 8: Indenter apparatus.

oriented along the surface normal over any location on the fingerpad. By sliding the indenter along the surface normal we can produce a desired inward displacement of the membrane at the contact location. This was done for a set of 25 points which were distributed over the entire fingerpad and whose coordinates had been previously measured. The indenter used was a metal rod with a diameter of $2.5mm$, designed to approximate a "point" indenter without damaging the latex membrane. The inward displacement at the contact was always kept at $0.5mm$. We indented the membrane at each of the chosen points and obtained the corresponding reconstructed grid. For each reconstruction, the centroid of the contact area was computed in order to identify the contact location. Finally, the coordinates of the contact location were compared with the actual coordinates of the point on the membrane that was in contact with the indenter. The norm of the resulting error vector had a mean of $0.75mm$. The maximum error was $1.9mm$, equal to one half of the distance between neighboring dots on the membrane surface.

Deformation Depth: Two different indenters were used to deform the membrane $1mm, 2mm, 3mm$ and $4mm$ along its surface normal at each of the 25 dots drawn on the membrane. In addition to the "point" indenter, a $2.54cm$-diameter flat rigid disk was used to deform the membrane over a large area. In each case the indenter was normal to the surface, held steady by the apparatus used in the previous experiment. The reconstructed grid was used to compute the maximum inward displacement of the tactile surface, which was then compared to the actual displacement effected by the indenter. Tables 1 and 2 show the mean and standard deviation of the error for each indenter and displacement.

The accuracy of the sensor degraded as the deformation

Displacement (mm)	Mean error (mm)	Std. deviation
1	0.1806	0.2486
2	0.3895	0.3099
3	0.8228	0.4091
4	1.5930	0.6613

Table 1: Point indenter.

Displacement (mm)	Mean error (mm)	Std. deviation
1	0.2444	0.2472
2	0.5356	0.4074
3	0.9489	0.6094
4	1.4700	0.4994

Table 2: Flat indenter.

depth increased. This was to be expected because large membrane deformations violate the assumptions of the reconstruction algorithm. The above errors can be used to calibrate subsequent sensor measurements.

Estimation of Local Curvature: Using three different indenters, a deformation of $4mm$ was applied along the surface normal, near the center of the fingerpad and the reconstructed grid was obtained. This process was repeated twenty times. The three indenters used were the "point" and flat indenters described above, as well as a $1.27cm$-diameter sphere. For each reconstructed grid, we identified the membrane location that was maximally displaced. At that point of maximum displacement, we numerically computed the rate of change of the surface tangent along two vectors that formed a local basis for the surface. The tangents' rate of change provided an estimate of local curvature at the contact. Table 3 shows the mean and standard deviation for each group of estimates. These means are

Indenter	Mean (cm^{-1})	Std. Deviation
Point	0.53	0.01
Ball	0.47	0.02
Flat	0.20	0.01

Table 3: Curvature measurements.

to be compared with the actual curvatures of the indenters which were 0 for the flat disk, $0.79cm^{-1}$ for the ball and $3.94cm^{-1}$ for the point indenter. The comparison shows poor agreement, due to the fact that the reconstructed grid was twice differentiated numerically and also because significant membrane deformation was required to effect a large enough contact area from which curvature information could be extracted. Despite their low accuracy, the estimates in Table 3 do exhibit the right trend and can be used to distinguish between different curvatures, albeit with rather coarse quantization.

The accuracy of the curvature measurements can be improved by sampling the membrane surface more densely (drawing and imaging a denser grid of dots). It should be noted that the curvature estimates for the point and ball indenters are comparable partly because the membrane cannot deform perfectly around the point indenter, making it indistinguishable from a variety of slightly larger conical indenters.

5 Conclusions and Future Work

We have presented the results of tactile sensing experiments with a new, deformable, gel-filled tactile sensor. Previous work (Shimoga & Goldenberg) has shown the superiority of gel fingertips for force dissipation and conformability. Our sensor reconstructs the *shape* of an elastic membrane using image data, thus providing a rich set of tactile information. The experiments presented here demonstrated the performance of this sensor in simple tasks involving contact localization, spatial resolution, contact depth and curvature discrimination. For small deformations of the membrane, the contact localization error was less than $0.1mm$ over a $4cm^2$ area, while the spatial resolution was better than $2mm$. The sensor can accurately determine deformation depth for small deformations. Curvature estimation is monotonic, however the estimates suffer from the low resolution of the numerical data used to compute derivatives.

The experiments discussed here involved geometrically-defined idealized tasks. Results on the use of our sensor in manipulation experiments are presented in [16]. Other applications being explored include the miniaturization of the sensor and use as a laparoscopic device in minimally-invasive surgery. Future work may include the inclusion of a load cell within the sealed membrane in order to better estimate membrane and contact forces.

References

[1] S. Begej. Planar and finger-shaped optical tactile sensors for robotic manipulation. *IEEE Transactions on Robotics and Automation*, 4(5):472–484, 1988.

[2] A. D. Berger and P. K. Khosla. Using tactile data for real-time feedback. *International Journal of Robotics Research*, 10(2):88–102, April 1991.

[3] D. M. Brock and J. K. Salisbury. Implementation of behavioral control on a robot hand/arm system. In *Proc. of the 1991 IEEE International Conference for Robotics and Automation*, June 1991.

[4] D.M. Brock and S. Chiu. Environment perception of an articulated robot hand using contact sensors.

In *Robotics and Manufacturing Automation*, pages 89–96. vol 15 of PED, ASME Winter Annual Meeting, November 1985.

[5] R. W. Brockett. Robotic hand with rheological surfaces. In *Proc. of the 1985 IEEE International Conference on Robotics and Automation*, pages 942–946, 1985.

[6] A.S. Collins and W.A. Hoover. A prototype for an image-based tactile sensor. In *Proc. of the 1987 IEEE International Conference for Robotics and Automation*, pages 1760–1765, June 1987.

[7] M.R. Cutkosky and I. Kao. Computing and controlling compliance of a robotic hand. *IEEE Transactions on Robotics and Automation*, 5:151–165, 1989.

[8] B.S. Eberman and J.K Salisbury. Determination of manipulator contact information from joint torque measurements. In *Experimental Robotics I, The first Intl. Symposium*, pages 2221–233. Lecture Notes in Control and Information Sciences, Springer-Verlag, June 1990.

[9] R. S. Fearing. Tactile sensing mechanisms. *International Journal of Robotics Research*, 9(3):3–23, 1990.

[10] N. Ferrier, K. Morgansen, and D. Hristu. Implementation of membrane shape reconstruction. Technical Report 97-1, Harvard Robotics Lab, Harvard University, 1997.

[11] N. J. Ferrier and R.W. Brockett. Reconstructing the shape of a deformable membrane from image data. *Int. Journal of Robotics Research*, 1999 (under review).

[12] W.D. Hillis. Active touch sensing. *International Journal of Robotics Research*, 1(2):33–44, 1982.

[13] R.D. Howe. *Dynamic Tactile Sensing*. PhD thesis, Stanford University, Dept. of Mechanical Engineering, 1990.

[14] R.D. Howe. Tactile sensing and control of robotic manipulation. *Journal of Advanced Robotics*, 8(3):245–261, 1994.

[15] R.D. Howe and M.R. Cutcosky. The sliding of robot fingers under torsion and shear loading. In *Proc. of the 1989 IEEE International Conference for Robotics and Automation*, pages 103–108, June 1989.

[16] D. Hristu. *Optimal Control with Limited Communication*. PhD thesis, Harvard University, Div. of Engineering and Applied Sciences, 1999.

[17] J. Kerr and B. Roth. Analysis of multifingered hands. *International Journal of Robotics Research*, 4(4):3–17, Winter 1986.

[18] D. A. Kontarinis and R. D. Howe. Tactile display of vibratory information in teleoperated and virtual environments. *Presence*, 4(4):387–402, 1995.

[19] H. Maekawa, K. Tanie, and K. Komoriya. Tactile sensor based manipulation of an unknown object by a multifingered hand with rolling contact. In *IEEE International Conference for Robotics and Automation*, pages 743–750, June 1995.

[20] H. Maekawa, K. Tanie, K. Komoriya, M. Kaneko, C. Horiguchi, and T. Sugawara. Development of a finger-shaped tactile sensor and its evaluation by active touch. In *Proc. of the 1992 IEEE International Conference for Robotics and Automation*, pages 2221–233, June 1992.

[21] D. J. Montana. The kinematics of contact and grasp. *International Journal of Robotics Research*, 7(3):17–32, 1988.

[22] E. J. Nicolson and R.S. Fearing. Sensing capabilities of linear elastic cylindrical fingers. In *Proc. of the RSJ/IEEE International Conference on Intelligent Robots and Systems*, volume 1, pages 178–85, 1993.

[23] J. Rebman and K.A. Morris. A tactile sensor with electrooptic transduction. In A. Pugh, editor, *Robot Tactile Sensors*, volume 2, pages 145–155. IFS Publications, Springer-Verlag, Berlin, 1986.

[24] R.A. Russell. Compliant-skin tactile sensor. In *Proc. of the 1987 IEEE International Conference for Robotics and Automation*, pages 2221–233, June 1987.

[25] J.K. Salisbury. Interpretation of contact geometries from force measurements. In *Robotics Research: The first Int. Symp.* M.Brady and R.P. Paul, eds, Cambridge, MA: MIT Press, 1984.

[26] K.B. Shimoga and A.A. Goldenberg. Soft robotic fingertips part I: A comparison of construction materials. *Int. Journal of Robotics Research*, 15(4):320–334, 1996.

[27] K.B. Shimoga and A.A. Goldenberg. Soft robotic fingertips part II: Modeling and impedance regulation. *Int. Journal of Robotics Research*, 15(4):335–350, 1996.

[28] T. Speeter. A tactile sensing system for robotic manipulation. *International Journal of Robotics Research*, 9(6):25–36, 1990.